Response to Reviewer comments

We would like to thank both reviewers for their time, comments and suggestions for improvements. Basically, the two reviews are different in main aspects.

We think that both reviewers are right in the way they understand the paper.
Reviewer 1 agrees with our concept but criticises our application of fire emissions that is not suited for our concept.
In contrast, Reviewer 2 points out that the concept is not completely correct within the Lagrangian conceptual framework. However, for the specific case of fire emissions, Reviewer 2 raised the relevance of study.

Our new manuscript version is thoroughly revised. We adjusted our concept and think this new interpretation is in agreement with the Lagrangian framework. Furthermore, we replaced our application example of fire emissions and use effective emission injection heights as recommended by Reviewer 1. The adjusted concept is suited for this application, as raised by Reviewer 2, and the results better emphasise the relevance of the study.

Our response to the specific points are given below after the reviewer's remark in Italics. We start with Reviewer 2 as these comments introduced major revisions.

Reviewer comments 2

General comments

2.1 The paper "Assumptions on mixing heights influence the quantification of emission sources: A case study for Cyprus" intends to quantify the influence of varying boundary layer heights on the quantification of source contributions based on backward simulations performed with a Lagrangian Particle diffusion model (LPDM). In reality, however, this paper rather describes the influence of varying emission heights on the quantification of source contributions.

First of all, this comments points out that we mixed up the terms 'emission height' and 'mixing layer height'. Our use of the term 'mixing layer height' is misleading or even wrong as it describes the well-mixed layer of the PBL height (see also comment 2.3). The emission height defines the height where emission sources release pollutants to the atmosphere. The vertical mixing is then realised by turbulent processes up to the PBL height. This mixing layer dynamics is represented by the underlying meteorological model (more details in comment 2.2. and 2.4).
In case of fire emissions, this mixing layer dynamics is underrepresented as the fire-induced convection results in enhanced vertical mixing (details in comment 2.5 and 2.6).
Therefore, the reviewer is correct that we actually analysed the impact of varying emission heights for such a case.
However, the suggested title does not appropriately reflect our revised manuscript. We prefer to use the more technical term 'footprint layer' (FL) height instead of emission height which is widely used in the literature (e.g. Stohl et al., 2007a). This term offers more flexibility to describe any layer, in which emitted pollutants are assumed to affect tracer particles.
In our revised results, we consider two different cases:
In Section 3.1, we use the FL height to simulate the vertical mixing layer dynamics in the PBL height. This tests whether the tracer particles represent a well-mixed boundary layer (see also comment 2.4). In Section 3.2, we use the FL height to simulate the vertical mixing due to pyroconvection (see comment 2.5 and 2.6).
We adjusted our title using the new term footprint layer (FL) height and replaced the term 'mixing layer' with this new term throughout the whole manuscript.

Most relevant changes:
→ new title
→ new abstract
→ use of footprint layer (FL) height instead of mixing layer (ML) height
→ revised listing of methods in chapter: Methods 2.2

2.2 Looking at surface emissions (emission height <= 100 m), it is incorrect to assume that such emissions are taken up by particles that are within the mixing or boundary layer height. In the Lagrangian conceptual framework, such emissions are only taken up by the particles crossing this grid cell within the lowest model level, typically set to 0-100m.

We agree and have this made clear in the text, see comment 2.4.

2.3 Applications mentioned by the authors (like Stohl et al., 2007) are neither a simplification, nor do they assume constant mixing layer heights.

Yes, applications of FLEXPART do not use constant mixing layers, they use constant emission respective footprint layer heights. Our previous manuscript version uses the term in a misleading or even wrong manner. In the revised version, the term 'mixing layer' refers to the well-mixed layer of the atmosphere, such as realised in (convective) PBL heights.

2.4 In forward like in backward mode, the mixing layer dynamics is simulated in the model and thus does not need to be considered while counting the particles.

This is correct as already specified in 2.2. The tracer particles should be evenly distributed throughout a well-mixed PBL height, representing the vertical mixing. Within the PBL, the pick up of pollutants is therefore independent of the FL height assumption. It should be possible to assume any FL height up the PBL. Typically, the lowest model layer, 0-100m, is recommended as minimum FL height in LPDM applications. This height includes the emission height of surface sources and corresponds to the minimum PBL height that guarantees a well-mixed layer and a reasonable particle counting statistics. Therefore, the reviewer is right that considering particles above the lowest model layer is actually not necessary. In our analysis in Section 3.1, we test extreme cases of extending the FL to the entire mixing layer, represented by the PBL, by dynamically using the local PBL height as FL height.
We have implemented this interpretation in the introduction and also adapted our conclusions. Now, our findings show that a FL height following local PBL heights yields systematic differences, with daytime and night-time sensitivity differences. At daytime when a well-mixed convective PBL can be assumed, the differences indicate that residual inaccuracies occur in the representation of the mixing layer dynamics.

→ Introduction: page 2, line 23 – page 3, line 7
→ revised abstract
→ revised conclusions: page 13, lines 14-30

2.5 The framework, however, is different in case that the emission height exceeds the height of the lowest (surface) model layer, and especially in circumstances where emission heights are highly variable. This is especially the case for forest fire emissions, strongly depending on the dynamics of the fires and the temperatures prevailing in the plumes.

We are pleased that the reviewer supports the relevance of our study for the application on fire emissions.
Fires have their own dynamics and the fire-induced convection controls the vertical mixing of smoke constituents up to the injection height, which can exceed the PBL height and even reach the lower stratosphere. The mixing layer simulated in FLEXPART cannot account for this additional vertical transport. Thus using constant emission heights of 100m is only justified for surface emissions.
→ Introduction: page 3, lines 7-11

2.6 Here, the variable emission heights need to be considered by including particles from higher levels in the quantification of source contributions. In this case, the effects described by the authors are relevant.

This comment encouraged us to recalculate our application example with emission heights from the plume rise model (PRM) injection heights of GFAS (Remy et al., 2017).
We combine a 5 days' period during the strong fire event in August 2007 in Greece with one of our case studies that shows transport routes passing through this fire region. For this case study, the fire plume heights even exceed local PBL heights and represent pyroconvection. We find that a 300m FL height assumption overestimates the CO source contributions by 60%. We also calculated the source contributions for the constant 100m FL assumption and the for the PBL heights. The 100m FL height

assumption introduces an overestimation of 77% while the difference for PBL heights is more moderate with 30%. These relative and absolute differences are summarised in the new Table 3. We also revised Fig.6 (now Fig.7). It shows the time series of CO source contributions and the density-weighted residence time for all four FL heights assumption: 100m, 300m, PBL height and fire plume height. The constant 100m and 300m FL heights show similar but still discernible results which confirms that the results are only weakly sensitive to small changes in FL heights. Thus the mixing layer dynamics may still be sufficiently represented by the trajectories for many applications. The PBL height assumption can reproduce the CO peak during daytime when convective PBL heights are similar to fire plume heights. However, this PBL height assumption erroneously elevates the background for stable shallow PBL heights at night.
This new analysis even shows a strong overestimation of fire emission impact for the use of constant FL heights up to 300m. Here, the PBL height might even be a reasonable assumption for biomass burning wherever observation-based fire plume heights are not available. We think that these findings are an additional value and emphasize the relevance of the study.

→ modifications for use of fire plume heights in chapter: Methods 2.2 and 2.4
→ completely revised chapter: Results 3.2
→ new Table 3
→ revised Fig. 6 (former Fig. 5)
→ revised Fig. 7 (former Fig.6)
→ revised conclusions: page 13, line 31 – end
→ revised abstract

2.7 Therefore, these aspects should be properly discussed in a revised manuscript version, before the paper can be accepted.

We have introduced new simulations and adapted the text throughout the manuscript accordingly, see answers above.

Reviewer comments 1

General comments

1.1 The paper "Assumptions on mixing heights influence the quantification of emission sources: A case study for Cyprus" by Hueser et al. describes the impact of two different assumptions on the height of the mixing layer in a Lagrangian particle dispersion model which influence the emission sensitivity and hence the contribution of individual emission source locations to a local concentration enhancement. The paper itself is clearly structured, however in some cases it is difficult to follow the conclusions as some important classification of individual cases are not explicitly explained in the manuscript.

We are pleased that the reviewer noted a clear structure in our manuscript. The revision based on Review 2 (see above) introduced major changes and new conclusions. We hope this new manuscript version is easier to follow.

1.2 A key issue for my criticism is a missing or only roughly touched differentiation between boundary layer height and mixing height, as these two quantities are only describing the same effect for well mixed convective boundary layers.

This comment ties into Comments 2.1.-2.4. We have now updated the manuscript to make clear that all mixing except pyroconvection is represented in the trajectories. As explained above, we focus on studying the numerical method of using a footprint layer (FL) to (a) test the representation of mixing in the case of a well-mixed boundary layer and (b) represent the pyrogenic mixing up to fire plume heights. Thus we now differentiate between mixing height, boundary layer height and footprint layer height, and only assume that the boundary layer height equals the mixing height in the case of a convective boundary layer.
However, within the Lagrangian framework, the tracer particles are effectively mixed within the simulated PBL height (Stohl et al. (2005), Section 3 second last paragraph), even for stable conditions. (see also comment 1.3)
→ new title
→ use of footprint layer (FL) height instead of mixing layer (ML) height throughout the manuscript

1.3 The manuscript makes no distinct differentiation for boundary layer stability conditions. Stable, e.g. nocturnal or boreal winter inversion boundary layers are characterised by much lower vertical mixing or even downward mixing and the surface emission sources are not even mixed throughout the much more shallow boundary layer. For neutrally stratified boundary layers (e.g. nocturnal residual layers) also no vertical mixing takes places. Hence mixing layers as described in the paper are only representative for a fraction of the occurrence in boundary layer types. A better characterisation for the types of boundary layer, as well as a PDF of boundary layer heights along the major emission sensitivity paths (e.g. emission sensitivity larger than 0.5 or even larger than 0.1 sm^2kg^-1) would help to understand the conditions for the scenarios.

We agree with the reviewer concerning the conditions for vertical mixing for different PBL boundary layer stability conditions. Unfortunately, as already mentioned in comment 1.2, LPDMs evenly distribute the tracer particles within the PBL. This trajectory distribution represents the vertical mixing independently of the stability conditions. Also, a minimum PBL height of 100m is assumed that guarantees for minimum vertical mixing in stable conditions. Within the Lagrangian framework a discussion about vertical mixing in different PBL heights is thus limited.

Since the mixing layer dynamics is simulated in the model, our study rather tests the representation of this vertical mixing for the specific case of a well-mixed PBL. Furthermore, we only analysed systematic differences linked to the diurnal cycle of PBL heights. The differentiation of PBL heights only specifies convective PBL types at daytime and more stable types at night. As suggested by the reviewer, we present the variability of PBL heights for our single case study in a frequency distribution in the new Fig.1. 55% of PBL heights are above 300m and assumed to be represent convective PBL heights. 45% are below 300m and represent more stable conditions.
We hope that our added figure about the frequency distribution supports the analysis of our case study in Section 3.1.1.

→ revisions in: Results 3.1.1, page 8, lines 4-13
→ new Fig. 1

1.4: Another key criticism the choice of using fire emissions for the case study together with the concept of the mixing layer. As fires represent local heat sources, the conditions of vertical motion and mixing of fire emissions are very different from other emission sources. This is one of the reasons why for fires usually effective emission heights are assumed in modelling, as fires trigger dry convection or often even pyroconvection which results in a much more enhanced vertical mixing and hence uplifting of air masses with enhanced biomass burning tracers. Therefore, the mixing layer height is a not well chosen concept for this emission type.

We agree that that in the case of fire emissions the effective emission injection heights are better suited to represent the vertical distribution of pollutants. Especially, when the fire plume tops exceed the PBL height, the mixing layer dynamics simulated in LPDMs cannot account for the enhanced vertical mixing. Therefore, we recalculated the application example with fire plume top heights from the GFAS emission inventory. This suggestion is also in agreement to Reviewer 2 (see also comment 2.5 and 2.6). Our new analysis even shows a much stronger overestimation of emission impact for the use of constant FL heights up to 300m. These findings are an additional value to emphasize the relevance of the study.

→ modifications for use of fire plume heights in chapter: Methods 2.2 and 2.4
→ revised section 3.2
→ revised conclusions: page 13, line 31 – end
→ major changes in conclusions and abstract

1.5: These two aspects should be properly discussed in a revised manuscript version

We have differentiated PBL types in the manuscript text as far as this is compatible with the major revisions based on Review 2. We also follow the idea to use effective fire emission injection heights, recalculated our application example and adapted the conclusions accordingly.

1.6 The statistical significance of the findings should be analysed for at least the climatological values.

The study period of one month contains various weather and transport patterns which are not only typical for summertime conditions. This is now highlighted in Sect. 3.1.2, page 9 lines 26-32

Specific comments

Page 1, Line 19: "Local air composition is determined by transport processes....." This statement might be correct for locations which are far from emission sources. However, as a general statement this sentence is not correct, as local emissions and chemical production or destruction can be equally dominating the local air composition.

We should use the word ‘co-determine’ instead of ‘determine’. Revised form:
“Transport processes in the atmosphere co-determine local air composition as …”
→ page 1, line 21

Page 2, Line 5: "...of the dispersion of an air mass by turbulence and convection in the lower troposphere." As these processes cannot directly resolved by lagrangian models on scales larger than a few kilometres, a good representation of these processes cannot be achieved. Statistical fluctuations are used as a tool to capture the main effects of these processes, only.

This formulation is misleading and the content of the citation not presented correctly. Revised form:
“Since turbulence is stochastic a large number of trajectories should correctly represent the dispersion of an air mass in the lower troposphere (Stohl et al., 2002).”
→ page 2, lines 6-7

Chapter 2: The derivation of the equations is straight forward, such tha they could be moved to an appendix, with a much more shortened explanation of the terms which are displayed in the figures (e.g. EQ2 and 4 are so similar except for the summation boundary, EQ3 and 5 except for the index in the denominator. Only EQ10 and EQ11 are of importance for the further analysis and discussion.

We agree that the derivation is straight forward. However, we appreciate formulas to clarify our methods. Therefore, we just shorten the section containing formulas.

Page 7, line 30: What is the variability in PBL height? Here the PDF mentioned above would be a good way to illustrate this variability. Mean values usually do not help since they represent both daily and nocturnal conditions. However, as FLEXPART already provides the PBLH as output on the points of trajectory location, this information should be straight-forward to provide.

We expect a distinct variability for a case study with continental transport routes just because of a pronounced diurnal cycle in PBL heights over land surfaces. To clarify the variability, we added a plot of the frequency distribution for PBL heights during the 5 days’ simulation (see also comment 1.2).
→ page 8, lines 6-13

Page 8, line 5: This alternating pattern does not show a behaviour as expected from the change in diurnal and nocturnal boundary layer, which would result in larger areas with equal sign. Is this a consequence of the time integration? Are the differences statistically significant compared to the temporal internal variability?

This plot (new: Fig.2) is basically used as an introduction to the analysis. The time-integrated emission sensitivity is usually the standard application to localise and quantify emission sources.

Therefore, we use this application to show the differences in sensitivity when varying FL heights are used. This point is better emphasis ed in the revised version.
Furthermore, the time-integration sums up positive and negative sensitivity differences at single time steps, i.e. Fig 2b only shows the temporal net-effect. However, this spatial pattern has still a link to the diurnal cycle of emission heights. The trajectories spread over time and, therefore, pass distinct regions preferred over day or night. This is actually the background to further analyse the impact of temporal variations in PBL heights in the next paragraph.
→ page 8, lines 14-30

Page 8: Line 15 to 20: Why is in the last 24 hours the difference only in negative direction and does not exhibit a gain in emission sensitivity any more? Comparing to Fig.6a the last 24 hours correspond to an increase in CO gain over Greece, however, this is not visible in Fig.2.

The gain in emission sensitivity in the last 12 hours results from a PBL height that exceeds the 300m layer. This is obvious in Fig2b (now 3b) that indicates a gain in residence time in the last 12 hours. The strong dilution in the extended PBL height finally causes the loss in emission sensitivity. Actually, it's untypical that the PBL height exceeds the 300m layer in the last 6 hours (21-3 local time). Since the measurement site is located on a hilly ground at a distance of 10km to the coast, PBL heights are calculated in an inhomogeneous environment on a 0.2° grid. Thus, they suffer stronger uncertainties than above a homogenous surface. During the last hours, the trajectories get denser sharing the same grid cell and the calculated PBL heights are more sensitive to these uncertainties. Therefore, the effects during the last 12 hour, especially 6 hours, can exhibit an unexpected behaviour.
Fig. 6 (now Fig. 7) is completely new as we used different CO emission fluxes and fire plume heights. The time series shows a time window in the middle of the simulation period and is thus not comparable to Fig.2a (now Fig. 3a).

Tab.1: Here a distinction in PBLH > MLH and PBLH < MLH height would be helpful.

In the revised version, we do no longer use the term mixing layer height and refer to the term footprint layer height. We think, that it is not reasonable to adapt Table 1. This suggestion would be only valid for this specific case for a comparison to PBL heights. This table should also be applicable in a more general sense, for example, the comparison between constant FL heights and variable fire plume heights. Thus, the table generally lists the four possible effects of FL height changes.

Fig.3 and page 9 line 19-25: If the black line depicts the reference, it should be on the 0 line,as the difference of the reference to the reference is supposed to be zero. I would expect the black line to be the cumulative effect of all four processes, instead.

Thanks to the careful review. There is an error in the legend. The black line is the cumulative effect and not the 300m reference. The relative differences are calculated in reference to the emission sensitivity of the 300m layer. Thus, the reference is zero.

Technical points:

Page 8, line 20: time profile -> time series

This is modified in the revised version.

Page 9, line 32: Sentence structure appears wrong (verb is missing?).

A comma and a verb improves this sentence: “When PBL heights fall below 300m, the concentration of emitted mass flux is intensified and less trajectories are captured by the shallower layer.”

Page 11, line 24: ...both effects counteract with each other -> counteract each other

This is modified in the revised version.

Acknowledgements: This looks like a leftover from a preliminary manuscript version.

This is updated.

Section on data availability is missing.

A note about data availability is added at the end of the conclusions.

Assumptions on footprint layer~~mixing~~ heights influence the quantification of emission sources: A case study for Cyprus

Imke Hüser[1], Hartwig Harder[1], Angelika Heil[1], and Johannes W. Kaiser[1]

[1]Max Planck Institute for Chemistry, Mainz, Germany

Correspondence to: Imke Hüser (imke.hueser@mpic.de), Hartwig Harder (hartwig.harder@mpic.de)

Abstract. Lagrangian particle dispersion models (LPDMs) in backward mode are widely used to quantify the impact of transboundary pollution on downwind sites. Most LPDM applications count particles with a technique that introduces a so-called footprint layer (FL) with constant height, in which passing air tracer particles are assumed to be affected by surface emissions. ~~assume mixing of surface emissions in a boundary layer that is constant in height.~~ The mixing layer dynamics is represented by the underlying meteorological model. This particle counting technique implicitly assumes that the atmosphere is well-mixed in the FL. We have performed backward trajectory simulations with the FLEXPART model starting at Cyprus to calculate the sensitivity to emissions of upwind pollution sources. ~~The height of this mixing layer (ML), however, is subject to strong spatio-temporal variability. Neglecting this variability may introduce substantial errors in the quantification of source contributions. Here, we perform backward trajectory simulations with the FLEXPART model starting at Cyprus to quantify these errors. The simulations calculate the sensitivity to emissions of upwind pollution sources within the ML height.~~ The emission sensitivity is used to quantify source contributions at the receptor and support the interpretation of ground measurements carried out during the CYPHEX campaign in July 2014. Here we analyse the effects of different constant and dynamic FL height assumptions. ~~It is determined by two interacting factors: the dilution of pollutants within the ML and the number of trajectories impacted by the emissions. In this study, we calculate the emission sensitivity for a constant ML height of 300 m and a dynamical ML height to compare the resulting differences.~~ The results show that calculations with FL heights of $100\,\mathrm{m}$ and $300\,\mathrm{m}$ yield similar but still discernible results. Comparison of calculations with FL heights constant at $300\,\mathrm{m}$ and dynamically following the PBL height exhibit systematic differences, with daytime and night-time sensitivity differences compensating each other. The differences at daytime when a well-mixed PBL can be assumed, indicate that residual inaccuracies in the representation of the mixing layer dynamics in the trajectories may introduce errors in the impact assessment on downwind sites. ~~The results show that the impact of emission sources is predominantly overestimated by the neglected dilution in expanded daytime ML heights. There is, however, substantial variability in the simulated differences. For shallow marine or nocturnal ML heights, for example, a ML assumed to high may lead to an underestimation of the intensive concentrations. This variability is predominantly caused by the spatio-temporal changes in ML heights and the meteorological conditions that drive the dispersion of the trajectories.~~ Emissions from vegetation fires are mixed up by pyrogenic convection that is not represented in FLEXPART. Neglecting this convection may lead to severe over- or underestimations of the downwind smoke concentrations. Introducing an extreme fire source from a different year in our study period and using fire observation-based plume heights as reference, we find an overestimation of more than 60% by the constant FL height assumptions used for

surface emissions. Assuming a FL that follows the PBL may reproduce the peak of the smoke plume passing through but erroneously elevates the background for shallow stable PBL heights. It might thus be a reasonable assumption for open biomass burning emissions wherever observation-based injection heights are not available. ~~In an application example, the impact of CO emissions from hypothetical forest fires is simulated and source contributions are compared for different ML heights. The resulting difference shows that the 300 m overestimates the total CO contributions from upwind sources by 16%. Thus, it is recommended to generally implement a dynamic mixing layer height parametrization in LPDMs to prevent these errors.~~

1 Introduction

Transport processes in the atmosphere co-determine local air composition~~Local air composition is determined by transport processes in the atmosphere~~ as trace substances can be transported over thousands of kilometres by the wind (e.g., Forster et al., 2001). Long-range transport of pollutants can drastically impair air quality in downwind areas and can trigger exceedances of ambient air quality thresholds (e.g., Vardoulakis and Kassomenos, 2008; Poupkou et al., 2014; Lelieveld et al., 2015). Therefore, the identification of upwind emission sources and the quantification of their impact by atmospheric dispersion modelling is crucial for implementing effective air pollution abatement measures.

One of the main tools for analysing the transport pathways of air pollutants from their source regions to a measurement site are trajectory models. These models track the path of an air tracer particle forward or backward in time in order to establish relationships between the pollution source and the receptor site (Stohl, 1998). Following the recommendation of Stohl et al. (2002), the backward simulation with Lagrangian Particle Dispersion Models (LPDMs) are most suitable for the interpretation of atmospheric trace substances measurements. LPDMs calculate the trajectories of a large number of tracer particles in the mean wind and in statistically modelled turbulent fluctuations (Rodean, 1996; Stohl, 1998). Since turbulence is stochastic, a large number of trajectories should correctly represent the dispersion of an air mass in the lower troposphere~~This allows for a realistic representation of the dispersion of an air mass by turbulence and convection in the lower troposphere~~ (Stohl et al., 2002). Hence, LPDMs such as FLEXPART (Stohl et al., 1998; Stohl and Thomson, 1999; Stohl et al., 2005) are frequently used to identify source regions of pollution and to quantify their contributions to the atmospheric composition at a measurement site (e.g. Stohl et al., 2007a; Lal et al., 2014). Furthermore, these models are used in an inverse mode to estimate the source strength of emissions. Here, the emission fluxes are adjusted to optimise the agreement between simulated and observed concentrations (Stohl et al., 2009). This inverse method is also applied to validate or improve emission inventories of atmospheric species (Pan et al., 2014).

The methodology in LPDMs is based on the assumption that any regions passed by the trajectories can potentially affect the receptor site. Since emissions from surface~~pollution~~ sources are distributed over a vertical~~well-mixed~~ layer adjacent to the ground, only trajectories passing this so-called footprint layer (FL) (Stohl et al., 2007a) identify effective source regions. Thus, the source receptor relationship is derived from the trajectories' residence time within this well-mixed layer in the upwind area of influence as described in Seibert and Frank (2004). ~~Hence, the longer the trajectories reside in this FL height the more pollutants are picked up and transported to the downwind receptor site.~~ Following Seibert and Frank (2004), the trajectories' residence time in the FL height quantifies the source-receptor relationship for surface sources when any transport losses are ignored. This source-receptor relationship~~It~~ is a function of space and time that maps quantitatively the relative contribution of pollution sources per unit strength of the emission flux to the air composition at the receptor. Therefore, it is also termed 'footprint function', the 'source weight function' (Schmid, 1994; Kljun et al., 2002) or 'footprint emission sensitivity' (Stohl et al., 2007a)~~, the term used here.~~ Here, we refer to the general term 'emission sensitivity'.

~~The height of this well-mixed layer generally corresponds to the mixing layer (ML) height of the planetary boundary layer (PBL). This layer is characterized by turbulent processes and uniformly mixes conservative tracers with a time scale of about an hour or less (Stull, 1988).~~ Most~~Typically,~~ applications of source quantification~~identification~~ with LPDMs in backward mode assume constant FL~~use constant ML~~ heights of $100\,\mathrm{m}$ (e.g., Stohl et al., 2007a; Van Dam et al., 2013; Pan et al., 2014), $150\,\mathrm{m}$ (Duck et al., 2007) or $300\,\mathrm{m}$ (Lal et al., 2014). ~~This simplified assumption avoids to exceed PBL heights and to involve air masses of the free troposphere. Furthermore, the dilution of surface emission fluxes is constant and therefore the pollution emitted to the ML is constant per unit strength. With this simplification, the pick up of pollutants only depends on the residence time of trajectories within the ML height. The residence time in the ML is thus used to describe the relationship of the receptor concentration to emission surface flux of inert species (Seibert and Frank, 2004).~~ The $100\,\mathrm{m}$ assumption includes typical emission heights for most surface sources as road traffic or industry, that is the height at which pollutants are released to the atmosphere. Furthermore, this height corresponds to the minimum planetary boundary layer (PBL) height typically used in LPDMs. A FL height below this minimum mixing layer height is not recommended in order to obtain sufficient particles for a reasonable particle counting statistics (Stohl et al., 2007b). The vertical mixing of pollutants is linked to the dynamics of the PBL and, therefore, it is subject to strong spatio-temporal variability. For convective conditions, the PBL height reaches up to $2-3\,\mathrm{km}$ and the turbulence mixes emitted pollutants throughout the whole layer on timescales of $15\,\mathrm{min}$ (Stull, 1988, 2006). The PBL should be well-mixed and the trajectories evenly distributed within the PBL. In fact, LPDMs use the PBL height to determine the layer over which tracers are effectively mixed, even for stable conditions. The mixing layer dynamics is represented by the vertical distribution of trajectories. The simulation of source contribution from surface emissions is therefore not very sensitive to changes in FL height as long as the height is within the PBL height (Stohl et al., 2007b). ~~However, PBL heights are subject to pronounced spatial and temporal variability and can reach more than 2000 meters. The dynamical behaviour of the PBL height is thus in contrast to the assumption of a constant ML height with a few hundred meter. If the constant ML height assumptions is replaced by such a dynamic ML height, the emission sensitivity is modified~~ Basically, a change in FL height influences the emission sensitivity by two counteracting effects.

On the one hand, an increase in FL~~ML~~ height leads to a stronger dilution of emission fluxes over this layer - an effect that reduces emission sensitivity. On the other hand, a larger number of trajectories passes through a deeper FL~~ML with increased~~ height that increases the residence time for the pick up of pollutants - an effect that increases emission sensitivity. As long as these effects are balanced, it is sufficient to consider only particles up to the expected minimum mixing height (Seibert and Frank, 2004). This is in agreement to the findings in Pan et al. (2014) that different FL height assumptions up to $300\,\mathrm{m}$ have no significant impact on the pick up of surface pollutants. Theoretically, any FL height assumption up to the PBL height should be possible. However, the validity of such an assumption has not yet been analysed. Furthermore, this treatment is only justified for surface emissions. Fire emissions have varying emission heights due to their own dynamics. The fire-induced convection controls the vertical mixing of pollutants within the fire plume that can exceed PBL heights and even reach the lower stratosphere (Andreae et al., 2004; Damoah et al., 2006; Dahlkötter et al., 2014). Therefore, the mixing layer dynamics simulated in FLEXPART underestimates this vertical transport (Duck et al., 2007) and a constant FL height assumption within the PBL height is not justified.

The aim of this study is to quantify the impact of varying FL heights on the results of source quantification~~the errors associated with the assumption of a constant ML height~~. We use backward simulations with the LPDM model FLEXPART that were carried out during the CYPHEX ground campaign in July 2014 to study the source areas and transport routes of air pollution at Cyprus. In Section 2 we derive the emission sensitivity function from the simulations and introduce our modifications to calculate the sensitivity for a dynamical FL~~ML~~ height. Furthermore, we develop a method to compare the effects of different FL~~ML~~ height assumptions. In Section 3.1 we compare the emission sensitivity for a constant FL~~ML~~ height of $300\,\mathrm{m}$ and a dynamical height derived from local PBL heights. In an application example in Section 3.2, we simulate the CO contributions ~~that result~~ from hypothetical forest fires. Here, we replace the FL heights with the altitude of plume top and quantify the differences in source contributions. Finally, in Section 4 we summarise and discuss the results.

2 Method

2.1 FLEXPART simulations

We have performed backward simulations with the LPDM model FLEXPART 9.2 (Stohl et al., 2005) during the CYPHEX campaign. The FLEXPART model simulations have been driven by operational meteorological input data of the European Centre for Medium-Range Weather Forecasts (ECMWF) with $0.2° \times 0.2°$ spatial resolution (derived from T799 spectral truncation). The model domain extends from $20°$W to $70°$E and $20°$N to $70°$N covering Europe, northern Africa and western Asia. To provide a temporal resolution of 1 hour a combination of analyses at 00, 06, 12 and 18 UTC and short forecasts data at intermediate time steps was used. Backward simulations were started from the measurement point in the Northwest of Cyprus by releasing 10000 neutral inert air tracer particles during an 1 hour time interval which are followed as trajectories over 5 days.

The positions of the tracer particles are calculated on a 3-d grid with a horizontal resolution of $0.2°$ that corresponds to the resolution of the input data on the model domain. A vertical resolution of 58 layers is used extending from $100\,\mathrm{m}$ (minimum height of the planetary boundary layer (PBL) set in the model) to an altitude of $10000\,\mathrm{m}$. The height of the layers gradually increases from $20\,\mathrm{m}$ to $1000\,\mathrm{m}$. The temporal resolution corresponds to the input data and is available in hourly time steps within the simulation period of $120\,\mathrm{h}$. In total, 216 simulations covering 9th July 2014 00 UTC to 4th August 2014 21 UTC in 3 hour time steps were carried out. They cover the entire period of the measurement campaign.

The output of FLEXPART is a 4-d function of emission sensitivity (Stohl et al., 2007a), three space dimension plus time, derived from the positions of all trajectories. It describes the relation between any emission source that is passed by the trajectories and the concentration of the respective atmospheric substance at the receptor. Since atmospheric emissions are diluted by mixing in adjacent air, emission sources are specified as emitted mass per time and volume in units of $\mathrm{kg\,m^{-3}\,s^{-1}}$, denoted by q. Receptor concentrations are expressed in a conservative quantity as mass mixing ratios, specified by χ (unitless). Then, the emission sensitivity is determined by the sum of the residence time T of all trajectories in this adjacent volume of air divided by the local air density ρ in $\mathrm{kg\,m^{-3}}$ without transmission correction (Seibert and Frank, 2004)

$$\frac{\partial \chi}{\partial q_{ijkn}} = \frac{T_{ijkn}}{\rho_{ijkn}}. \tag{1}$$

It is computed in the predefined 3-d output grid that uses the indices i, j, k to specify the spatial position x_i, y_j, z_k in the centre of each grid box. The fourth index n determines the time step t_n within the simulation period. This emission sensitivity can be interpreted as a source-weight factor. It describes the source contribution to the mass mixing ratio at the receptor relative to the source strength when any transport losses are ignored.

In addition to the described standard output, FLEXPART provides the PBL height for all individual tracer particles at their geographical position at each time step. The PBL heights are calculated by the model according to Vogelezang and Holtslag (1996) and use the concept of the critical Richardson number that is based on surface sensible heat fluxes and surface stresses available from the ECMWF input data (Section 3 in Stohl et al., 2005).

2.2 Surface Emission Sensitivity

Since we are interested in area sources at ground level, the emission sensitivity for volume sources in Eq. 1 is slightly modified to derive the sensitivity to surface emissions. The emission flux of an area source q_A ~~in units of $\mathrm{kg\,s^{-1}\,m^{-2}}$~~ is diluted over a vertical layer adjacent to the ground, the footprint layer (FL)~~mixing layer (ML)~~ of height h, following $q = q_A\,h^{-1}$. With this assumption, all grid boxes of height $z_k \leq h_{ijn}$ are attributed to the mixing volume in the FL height and influenced by pollutants. Here we use a variable FL height h_{ijn} in space and time that is specified by the corresponding indices i, j, n. Then, the emission sensitivity S to surface area sources in units of $\mathrm{s\,m^2\,kg^{-1}}$ is obtained with the density-weighted residence time $\widehat{T}_{ijn}$ in this mixing volume as

$$\widehat{T}_{ijn} = \sum_{k=1}^{z_k \leq h_{ijn}} \frac{T_{ijkn}}{\rho_{ijkn}} \tag{2}$$

$$S_{ijn} = \frac{\widehat{T}_{ijn}}{h_{ijn}}. \tag{3}$$

In this study, we use different FL~~ML~~ heights and have implemented three~~two~~ methods:

- The first method uses the assumption of a constant FL~~ML~~ height ~~within the PBL height (Seibert and Frank, 2004)~~. Here, we choose a layer of $h = 300\,\mathrm{m}$ which is used in published studies~~that is close to the typically expected minimum of PBL heights~~. Additionally, this height is slightly above the PBL minimum in the model of $100\,\mathrm{m}$. This allows to analyse the case that the assumed FL height exceeds the PBL height. ~~Then, all grid boxes with height $z_k \leq h$ are attributed to the mixing volume. The emission sensitivity S to surface area sources is obtained from eq. 1 with the density-weighted~~

~~residence time $\widehat{T}$ in this mixing volume as~~

$$\cancel{\widehat{T}_{ijn} = \sum_{k=1}^{z_k \leq h} \frac{T_{ijkn}}{\rho_{ijkn}}} \qquad \cancel{(2*)}$$

$$\cancel{S_{ijn} = \frac{\widehat{T}_{ijn}}{h}.} \qquad \cancel{(3*)}$$

~~The emission sensitivity S in units of $\mathrm{s\,m^2\,kg}$ is proportional to the density-weighted residence time of all trajectories within the ML height. Even for spatial or temporal integration, the emission sensitivity is independent of the ML height.~~

– The second method is new in this study and uses a FL height h_{ijn} that is variable in space and time.~~dynamic ML height. This ML height h_{ijn} is variable in space and time and specified by the corresponding indices i, j, n. Then, eq. 2* and 3* are replaced by~~

$$\cancel{\widehat{T}_{ijn} = \sum_{k=1}^{z_k \leq hijn} \frac{T_{ijkn}}{\rho_{ijkn}}} \qquad \cancel{(4*)}$$

$$\cancel{S_{ijn} = \frac{\widehat{T}_{ijn}}{h_{ijn}}.} \qquad \cancel{(5*)}$$

With this dynamic FL~~ML~~ assumption, the emission sensitivity depends on local varying FL~~ML~~ heights. ~~It is hence not proportional to the density-weighted residence time, when spatially or temporal integrated. To implement this dynamic ML height, we~~ We use local PBL heights calculated by the FLEXPART model to implement this dynamic FL height. However, from the output of FLEXPART only PBL heights along the particles' trajectories are available. To obtain gridded PBL heights from all single particle positions, we adapt the methodology described in Stohl et al. (2005), Section 8.1~~section 11.1~~. ~~Their eq. (55) is modified and calculates~~ We modify their Eq. (50) and calculate the PBL height h on the spatio-temporal output grid

$$h = \sum_{p=1}^{N} (f_p \, h_p) \qquad (4)$$

with N being the total number of particles, h_p the PBL height of particle p and f_p the fraction of the particle attributed to the respective grid cell. To calculate this fraction, we use a uniform kernel with bandwidths of $0.2°$ that corresponds to the output grid.

– The third method is specifically developed for the application on fire emissions. It is based on the the plume rise model (PRM) injection heights from the Global Fire Assimilation System (GFAS) (Rémy et al., 2017; Paugam et al., 2015). These fire observation-based plume heights are used as a variable FL height to simulate the emission impact of fire emissions provided by the GFAS (Kaiser et al., 2012).

2.3 Analysing the impact of footprint layer height assumptions

To analyse the impact of footprint layer (FL)~~ML~~ height variations, we calculate the emission sensitivity for ~~both~~ constant and dynamic FL~~ML~~ heights and analyse their differences. The absolute difference is described by

$$\Delta S_{ijn} = S_{ijn}(h_{ijn}) - S_{ijn}(h). \tag{5}$$

Here, ΔS_{ijn} is defined such that it is positive when FL~~ML~~ height differences introduce a higher emission sensitivity compared to the constant $300\,\mathrm{m}$ FL~~ML~~ height assumption. Differences in FL~~ML~~ height are determined in the same way, $\Delta h_{ijn} = h_{ijn} - h$, with positive sign for an increase.

To analyse the changes in emission sensitivity that are introduced by varying FL~~ML~~ heights, Eq. 3~~5*~~ is differentiated with respect to h,

$$\cancel{\frac{dS(h)}{dh} = \frac{d}{dh}\frac{\widehat{T}(h)}{h} = \frac{1}{h}\frac{d\widehat{T}}{dh} - \frac{1}{h^2}\widehat{T}.} \tag{8*}$$

~~Rearranging the equation to~~

$$\frac{dS(h)}{dh} = \frac{\widehat{T}}{h}\frac{1}{dh}\left(\frac{d\widehat{T}}{\widehat{T}} - \frac{dh}{h}\right). \tag{6}$$

~~and discretising~~ Discretising the differentials results in the simple relation

$$\frac{\Delta S}{S} = \frac{\Delta\widehat{T}}{\widehat{T}} - \frac{\Delta h}{h}. \tag{7}$$

The relative change in density-weighted residence time $\left|\frac{\Delta\widehat{T}}{\widehat{T}}\right|$ describes the gain / loss in impact since a deeper FL~~ML~~ height can capture more trajectories. The second term describes the relative change in FL~~ML~~ height $\left|\frac{\Delta h}{h}\right|$. It quantifies the dilution of emitted substances and represents the gain / loss in concentration. Thus, to describe the relative change in emission sensitivity, we need to analyse the overall difference of both effects. Additionally, both effects are coupled and interact with each other. An increase in FL~~ML~~ height results in an increase in residence time and is accompanied by a stronger dilution. Hence, the changes in emission sensitivity are the result of the counteracting effects: gain in impact and loss in concentration (dilution effect). It is crucial~~Crucial is~~ which of both turns out to be the dominating effect. This interaction is described in a case-by-case analysis presented in Tab. 1 ~~respectively~~ for increasing and decreasing FL~~ML~~ heights, respectively.

Following this case-by-case analysis, the overall difference in emission sensitivity, spatially and / or temporally integrated, is the result~~s~~ of these four characteristic differences

$$\underbrace{\Delta S_{tot}}_{\text{overall difference}} = \underbrace{\Delta S^{-}\left(\Delta h^{+}\right)}_{\text{dilution effect } <0} + \underbrace{\Delta S^{+}\left(\Delta h^{+}\right)}_{\text{gain in impact } >0} + \underbrace{\Delta S^{+}\left(\Delta h^{-}\right)}_{\text{gain in concentration } >0} + \underbrace{\Delta S^{-}\left(\Delta h^{-}\right)}_{\text{loss in impact } <0}. \tag{8}$$

Here, $\Delta S^{\pm}$ respectively $\Delta h^{\pm}$ are defined according to

$$\Delta X^{+} = \begin{cases} \Delta X & ,\Delta X > 0 \\ 0 & ,\Delta X < 0 \end{cases} \tag{9}$$

Table 1. Subdivision of the difference in emission sensitivity ΔS caused by FL~~ML~~ height variations Δh assigned to their dominating effects.

cases of interaction	dominating effect	
$\Delta h > 0$ and $\Delta S < 0$	$\left\lvert\frac{\Delta\widehat{T}}{\widehat{T}}\right\rvert < \left\lvert\frac{\Delta h}{h}\right\rvert$	loss in concentration (stronger dilution)
$\Delta h > 0$ and $\Delta S > 0$	$\left\lvert\frac{\Delta\widehat{T}}{\widehat{T}}\right\rvert > \left\lvert\frac{\Delta h}{h}\right\rvert$	gain in impact
$\Delta h < 0$ and $\Delta S > 0$	$\left\lvert\frac{\Delta\widehat{T}}{\widehat{T}}\right\rvert < \left\lvert\frac{\Delta h}{h}\right\rvert$	gain in concentration (less dilution)
$\Delta h < 0$ and $\Delta S < 0$	$\left\lvert\frac{\Delta\widehat{T}}{\widehat{T}}\right\rvert > \left\lvert\frac{\Delta h}{h}\right\rvert$	loss in impact

and

$$\Delta X^{-} = \begin{cases} 0 & ,\Delta X > 0 \\ \Delta X & ,\Delta X < 0. \end{cases} \tag{10}$$

The contributions interfere with each other and can buffer the overall difference. However, the individual contributions account for the variability that is introduced by changes in FL~~ML~~ heights. The negative and positive contributions span up a margin that envelopes the overall difference. A narrow or vanishing margin indicates a balance of the counteracting effects and little impact on the emission sensitivity. Therefore, this margin is a simplified tool to quantify the potential of errors in source analysis induced by a FL height assumption and uncertainties in the representation of vertical mixing ~~that rely on a constant ML height~~.

2.4 Simulation of CO source contributions

The fields of emission sensitivity S_{ijn} on the spatio-temporal output grid (spatial indices: i, j, temporal index: n) derived from the FLEXPART simulations have been calculated for inert substances. Therefore, it quantifies the relative source contribution from any emitted species that are conserved on time scales used here, such as for example carbon monoxide. To derive the absolute source contribution from CO emission sources, we need an additional field of CO emission mass flux density on the spatio-temporal grid, q_{ijn}^{CO} in $\mathrm{kg\,s^{-1}\,m^{-2}}$. Folding the sensitivity with the emission flux density and temporal integration results in a new field of potential CO source contributions

$$\chi_{ij}^{\mathrm{CO}}(t) = \sum_{n} (S_{ijn}(t) \cdot q_{ijn}^{\mathrm{CO}}). \tag{11}$$

χ_{ij}^{CO} is a unit less quantity and describes the CO contribution from the respective grid cell to the measured CO mass mixing ratio at the receptor point at time t. Therefore, it is used to identify the geographical distribution of sources and their impact. In general, a strong impact is expected if enhanced emission sensitivity encounters a strong emission flux. However, if errors in calculated emission sensitivities encounter strong local emission sources, the error in source contributions is expected to increase.

Spatial integration finally results in the total mass mixing ratio that is transported to the receptor. It represents the CO contribution due to transport process and should be quantitatively comparable to the measured enhancement over the typical background concentration χ_0 (Seibert and Frank, 2004; Stohl et al., 2007a). The observed CO mass mixing ratio χ_{obs} at the receptor at time t is thus the sum of the background mass mixing ratio and the transport contribution

$$\chi_{obs}(t) = \chi_0 + \sum_{i,j}\sum_{n}(S_{ijn}(t)\cdot q_{ijn}^{\mathrm{CO}}) + \epsilon. \tag{12}$$

The uncertainty ϵ accounts for older CO contributions prior to the simulation period, for unknown CO sources and model errors such as neglected transport losses.

In this study, we use the Global Fire Assimilation System GFAS1.2 (Kaiser et al., 2012) to quantify the CO source contributions from biomass burning of forest fires to the CO concentration at Cyprus during the CYPHEX campaign. We explicitly use the corresponding fire observation-based altitude of plume top (Rémy et al., 2017) to derive a dynamical footprint layer (FL) height that accounts for pyroconvection in the fire spots. The CO source contributions are calculated for this dynamical FL height and a constant FL height of $300\,\mathrm{m}$. Additionally, the CO contributions for the $100\,\mathrm{m}$ FL height and the PBL height are considered for an extended comparison. ~~These CO source contributions are calculated for both, the constant ML height of $300\,\mathrm{m}$ and a dynamic ML height. Furthermore, the differences are compared and analysed as described for the emission sensitivity in section 2.3.~~

However, in the period of the campaign, fire intensity was to weak to influence the CO concentration significantly. To analyse the impact of errors in calculated emission sensitivities, a strong fire event is necessary. Thus, we use a ~~5 days~~ CO emission pattern of a large biomass burning event that occurred in Greece, ~~in~~ 24-28 August 2007 ~~(Poupkou et al., 2014) to represent such a hypothetical strong fire event~~. During this period Greece suffered the worst forest fires in the past 50 years (Poupkou et al., 2014).

3 Results

3.1 Differences in emission sensitivity

3.1.1 A single case study

First we analyse the impact of footprint layer (FL)~~ML~~ height variations in a case study of the 19th July 2014 00 UTC+03 ~~with a pronounced diurnal cycle in PBL height~~. This case study describes the transport of air masses from South East Europe to Cyprus on a continental transport route during the five previous days. For transport routes along land masses, we can expect a pronounced diurnal cycle in PBL heights with peaks during daytime up to $2-3\,\mathrm{km}$ and the lowest layers about $100-300\,\mathrm{m}$ at night. ~~Typically, the PBL height peaks during daytime over heated land masses and reaches heights up to $2-3\,\mathrm{km}$. After sunset the layer collapses down to $100-300\,\mathrm{m}$ or even lower when surfaces cool down. Therefore, when compared to a constant ML height assumption of $300\,\mathrm{m}$, the error to local PBL heights is positive over day and negative over night. These differences in ML height introduce changes in emission sensitivity following Eq. 7 and thereby influence the simulation of upwind source~~

~~contributions. To analyse this, we chose the simulation of the 19th July 2014 00 UTC as a case study. It describes the transport of air masses from South-eastern Europe to Cyprus on a continental transport route. Thus, a distinct variability in PBL heights can be expected.~~ This variability in PBL heights during 5 days of transport time is analysed in a frequency distribution in Fig. 1. PBL heights above $300\,\mathrm{m}$ are assumed to to represent well-mixed convective PBL heights while heights below $300\,\mathrm{m}$ are characterised by less vertical mixing in more stable conditions. A minimum vertical mixing, however, is assumed within the PBL minimum of $100\,\mathrm{m}$ set in the model. The probability for the occurrence of a PBL height within $300\,\mathrm{m}$ is about 45%. Constant FL height assumptions in this range can compensate for an underrepresentation of vertical mixing in the trajectories. 55% of PBL heights exceed the $300\,\mathrm{m}$ that can influence the emission sensitivity, so that the analysis depends on a realistic representation of vertical mixing in the trajectories.

As a starting point, we analyse the emission sensitivity for ~~the upwind emission sources are identified using~~ the constant $300\,\mathrm{m}$ FL~~ML~~ height. By using a constant FL height, the emission sensitivity only depends on the changes in the (density-weighted) residence time since the dilution of emission flux is constant. Therefore, we integrate the emission sensitivity S_{ijn}, following Eq. 3, in time. ~~In a first step, the horizontal field of emission sensitivity S_{ijn}, following Eq. 3*, is integrated in time.~~ The resulting~~Then, the~~ 2-d field is mapped as shown in Fig. 2~~1~~a and indicates regions of enhanced sensitivity by colours. The higher the sensitivity values~~,~~ the higher the contribution of a source area~~an area source~~. ~~Hence, they identify upwind source regions and quantify their impact on the measurement site.~~

This method is typically used in LPDM applications to localise hotspots of upwind emission sources and to quantify their impact on the measurement site. For this standard application, we compare the emission sensitivities for the $300\,\mathrm{m}$ FL height and local varying FL heights realised by PBL heights. Following Eq. 7, the difference ΔS_{ijn} depends on the combined effect of changes in (density-weighted) residence time and in the dilution of emission flux. According to the $300\,\mathrm{m}$ standard application, we integrate ΔS_{ijn} in time. Since ΔS_{ijn} can be positive and negative over the course of the day, confer Tab. 1, the obtained 2-d field represents the net effect during the 5 days simulation period. It is shown in Fig. 2b and indicates the relative differences in emission sensitivity compared to Fig. 2a. ~~The next step is to analyse the differences in emission sensitivity that result from local varying PBL heights. First, the temporal variability is neglected and the differences ΔS_{ijn} are integrated in time. The obtained 2-d spatial field is shown on a map in Fig. 1b. It indicates relative differences in emission sensitivity compared to the application of the $300\,\mathrm{m}$ ML height. Thus, it quantifies the relative difference in reference to the local source strength.~~

In this example, the spatial distribution ~~of differences in emission sensitivity~~ exhibits a pattern of positive~~red~~ and negative values~~blue colors~~. Thus, the application of the constant $300\,\mathrm{m}$ FL height causes both an over and an underestimation of emission sensitivity compared to local PBL heights. However, the time-integrated differences represent the net effect over 5 days. In fact, the differences at single time steps can be larger. Here~~In fact~~, the ‘fixed’ FL~~ML~~ height application~~assumption~~ capitalises on over- and underestimations~~these local maxima and minima~~ compensating for each other. ~~Therefore, a systematic trend based on any spatial surface properties is not given.~~ The remaining net effect reveals an alternating spatial pattern. This is linked to the diurnal cycle of the PBL height since the trajectories pass distinct regions preferred at day or night-time.

Therefore, we~~To further~~ explore the impact of temporal variations in FL~~ML~~ height respective PBL heights and ~~, the emission sensitivity is~~ spatially integrate~~d~~ the emission sensitivity. Then, it only depends on time and its evolution can be represented in a simple time series~~profile~~ over the simulation period. For a comparison, this time series~~profile~~ is calculated for the emission sensitivity of the constant 300 m FL~~ML~~ height and local PBL heights as shown in Fig. 3~~2~~a. The colour of the filled areas indicates the sign of the difference and represents a regular alternating pattern. This results from~~is the result of~~ the characteristics of a diurnal cycle that leads to a pronounced temporal dependency. During daytime, the changes in PBL height introduce a loss in emission sensitivity and a gain over night. This suggests that stronger dilution in daytime FL~~ML~~ heights reduces the emission sensitivity, even though more trajectories are influenced by emissions. To further analyse this effect, the density-weighted residence time $\widehat{T}$ (Eq. 2)~~see Eq. 2* and 4*~~ of all trajectories within the FL~~ML~~ height is integrated in time. The time series is shown in Fig. 3~~2~~b for the constant 300 m FL~~ML~~ height and the varying PBL height with differences identified by colours. The different colours indicate a strong gain in residence time during daytime and a loss at night that correlates with the diurnal cycle of PBL heights. Furthermore, the comparison of both time series in Fig. 3~~2~~ points out that the gain in residence time over day is linked to a loss in emission sensitivity. Consequently, the dilution compensates for the gain in impact and vice versa. Averaged over the whole time period, the loss in emission sensitivity dominates by $-4\,\%$. However, this mean value covers smaller positive differences that occur at night time.

To account for the local and temporal variability in more detail, the overall difference is subdivided in contributions of the individual effects following Eq. 8~~11~~ and Tab. 1. Theoretically, when PBL heights exceed the constant 300 m FL~~ML~~ height assumption, the emission sensitivity can either decrease or increase. In this example, the stronger dilution predominately compensates for the gain in impact over the whole period. This effect contributes by $-8.8\,\%$ to the overall difference in emission sensitivity. However, in a few cases the dilution effect effect is less dominant and the gain in impact causes a positive contribution of 2.2%. When the PBL heights fall below 300 m, the described effects are reversed. Then, an increase in emission sensitivity by 6.2% is observed due to the intensified concentration in shallow FL~~ML~~ heights. However, when the loss in impact is stronger than this concentration effect, the emission sensitivity decreases. This effect contributes by $-3.6\,\%$ to the overall difference.

By merging these four separated effects, a margin between $-12.4\,\%$ to $+8.4\,\%$ is spanned. This margin envelopes the mean difference in emission sensitivity of $-4\,\%$ and represents the effects of local and temporal variability. Therefore, FL height changes within the PBL height are not buffered and result in over and underestimations in source contributions compared to a constant 300 m FL height assumption. ~~source contributions from emissions can be over and underestimated, when the constant 300 m ML height assumption is used.~~

3.1.2 Analysing the whole set of case studies

The analysed case study is only representative for a specific synoptic situation. We extend the analysis on the whole available set of 216 cases studies to account for a variety of synoptic situations. ~~The analysed single case study points out that changes in emission sensitivity result from the competing effects of dilution and gain in residence time. While the dilution only depends on local ML heights, the residence times of captured trajectories additionally depends on the vertical distribution of air tracers. Hence, it is controlled by the meteorological conditions during transport. To account for a variety of synoptic situations, the analysis is extended on the whole available set of 216 case studies.~~ Typically in summertime, a dominant pattern of northerly winds is expected in the Eastern Mediterranean that drives the transport of continental air masses from Eastern Europe. However, four distinct periods of west and south westerly flow in the Eastern Mediterranean were observed in July 2014 that cut off the expected continental transport routes and brought maritime air to Cyprus (Tyrlis et al., 2015). These unseasonal wind patterns offer a wide variety of synoptic situations. The analysis for the whole set of case studies is therefore not only representative for typical summertime conditions. ~~These alternating wind pattern offer a variety of meteorological conditions.~~

To compare different case studies, the procedure of the previous section, following Eq. 8~~11~~, is applied. For each case study, the overall and the margin of individual differences in emission sensitivity is calculated. The results are shown in a time series~~profile~~ over the period of the CYPHEX campaign in Fig. 4~~3~~. Here, the individual contributions are specified by different colours and envelop the overall difference as an uncertainty margin. By representing the temporal evolution over the time period of a month, changes on the temporal scale of days and weeks are involved. Therefore, this overview accounts for the impact of different synoptic patterns.

At first sight, it is obvious that negative differences dominate with mean values around $-5\,\%$. However, the wide margin points out that the variability allows for differences of $10\,\%$ and even more in both directions. For a detailed discussion, the differences are calculated as a mean over all 216 simulations combined with the interquartile range. The results are summarised in a box-whisker plot in Fig. 5 ~~4~~ and corresponding values of mean values, box and whisker ranges listed in Table 2. The box-whisker plot represents the spreading of data points and can be used to quantify the impact of each effect. Additionally, it accounts for the variability and includes single outliers that occur in changing synoptic conditions.

The detailed analysis of all case studies shows~~confirms~~ that the use of a variable FL height within the PBL lowers the emission impact ~~impact of emission sources is predominately overestimated during summer at Cyprus, when a constant 300 m ML height assumption is used~~. During summer at Cyprus, the $300\,\mathrm{m}$ FL height assumption predominately overestimates the emission sensitivity. For most simulations, the FL height differences ~~differences in ML height~~ introduce an overall mean difference in emission sensitivity between -2.8 and $-7.4\,\%$. This negative effect is mainly driven by the neglected dilution in PBL heights that frequently exceed the $300\,\mathrm{m}$ footprint~~ML~~ height assumption. For the majority of case studies, the dilution effect dominates the gain in impact and contributes with $6-11\,\%$ negatively to the mean overall difference. However, this changes when air tracers agglomerate above the standard $300\,\mathrm{m}$ footprint~~ML~~ height and thereby are captured by the overlying PBL height. Then, the gain in impact dominates and leads to an increase in emission sensitivity of about $2-3\,\%$.

When PBL heights fall below $300\,\mathrm{m}$, the concentration of emitted mass flux is intensified and less trajectories are captured by the shallower layer. This gain in concentration counteracts the decreasing residence time and contributes by $4-9\,\%$ to the difference in emission sensitivity. However, this is reversed, when the air tracers agglomerate between 100 and $300\,\mathrm{m}$ height that co-occurs with a shallow PBL height of about $100\,\mathrm{m}$. Such conditions typically occur when hot continental air masses reach the relatively cooler sea surface and travel slightly above the shallow marine PBL height. Then, the air tracers are captured by the $300\,\mathrm{m}$ FL~~ML~~ height assumption, even though they are in the free troposphere. According to this, a lower FL~~ML~~ height decreases the emission sensitivity due to a loss in impact. This negative effect contributes about $4-8\%$. However, the strong outliers of up to $-20\,\%$ represent a pronounced variability of this difference. This variability emphasis~~z~~es the risk of a false identification of emission sources within the constant $300\,\mathrm{m}$ FL~~ML~~ height.

Table 2. Mean values and calculated intervals in per cent for the interquartile range and the 2nd to 98th percentile as shown in the box whisker plot in Fig.5.

effect	mean	25%-75% box range	2%-98% whisker range
dilution	-8.5	$[-10.6\,,\,-6.1]$	$[-14.1\,,\,-2.7]$
gain in impact	$+2.6$	$[+2.0\,,\,+3.2]$	$[+1.0\,,\,+4.4]$
loss in impact	-6.1	$[-7.5\,,\,-3.6]$	$[-19.9\,,\,-1.5]$
gain in concentration	$+6.9$	$[+4.1\,,\,+8.9]$	$[+1.5\,,\,+16.7]$
overall	-5.0	$[-7.4\,,\,-2.8]$	$[-11.8\,,\,+4.2]$

Overall, a negative difference in emission sensitivity is observed. However, 21 positive outliers with a maximum of $9\,\%$ were found among the 216 simulations and the 98th percentile represents a positive difference of $+4.2\,\%$. This variability limits a distinct statement regarding the sign of errors that is introduced by FL~~ML~~ height variations. Hence, the $300\,\mathrm{m}$ FL height assumption can over and underestimate the impact of emission sources depending ~~impact of emission sources can be over- and underestimated and depends~~ on local PBL heights and meteorological conditions.

3.2 Differences in source contributions

3.2.1 Application - Simulation of extreme, localised CO source contributions

In this section, we analyse the impact of specific emission sources. This impact depends on the emission sensitivity and, additionally, on the local distribution and source strength of pollutants. We calculate the CO source contributions from forest fires as described in Section 2.4 for the $300\,\mathrm{m}$ FL height and for the specific fire plume top heights. During August 2007 strong forest fires occurred in Greece with the highest CO emissions on the 26th of August as shown in Fig. 6a. We combine the 5 days period from 24-28 August 2007 with the simulation of 26-30th July 2014 that shows transport routes passing through the fire regions. This is indicated in the corresponding map of temporal integrated emission sensitivities based on the constant $300\,\mathrm{m}$ FL height in Fig. 6b. ~~The analysis in the previous section reveals that the assumption of a constant 300 m ML height over and underestimates the sensitivity to emission sources. However, the impact of upwind emission sources additionally depends on the local distribution and source strength of pollutants. To analyse these errors, we simulate the CO source contributions from emissions of forest fires as described in section 2.4. The strong CO emissions in Greece during August 2007 are shown in Fig. 6a. Furthermore, the simulation of 30th July 2014 shows transport routes that pass the fire regions. This is indicated in the corresponding map of temporal integrated emission sensitivities based on the constant 300 m ML height in Fig. 6b.~~ Hence, a pick up of CO emissions and impact at the receptor can be expected in this hypothetical case.

The spatial distribution of CO source contributions is calculated following Eq. 11~~14~~ and shown in Fig. 6~~5~~c. In total, the Greek forest fires cause a CO contribution of $676\,\mathrm{ppb}$~~58.8 ppb~~ in the simulation. This is an order of magnitude larger than typical ~~would be a significant enhancement on top of the~~ background CO values at Cyprus of approximately $70\,\mathrm{ppb}$ which is the minimal value measured during the CYPHEX campaign (personal correspondence Uwe Parchatka) in unpolluted air. Nevertheless, the CO enhancement is a realistic value for this extreme fire event in Greece 2007. Poupkou et al. (2014) show similar enhancements in their model simulations for this specific fire event.

For these extreme fires the emission heights significantly exceed the $300\,\mathrm{m}$ FL height. On the 26th of August 2007, the altitude of fire plume top is between $1-3\,\mathrm{km}$ and is used to represent the FL height. We also calculate the CO source contributions that result from the fire plume heights. The absolute differences compared to the $300\,\mathrm{m}$ FL height are integrated in time and the spatial distribution is represented in Fig. 6d by different colours. Since only negative values are found over Greece, the FL height variations cause an overestimation of the CO concentration at the receptor. This overestimation sums up to a total difference of $-254\,\mathrm{ppb}$ or $60\,\%$ compared to the simulated CO contribution of $422\,\mathrm{ppb}$ for fire plume top heights. Accordingly, the stronger dilution in the deeper fire plume height is the major effect and dominates the gain impact in this hypothetical height. ~~To analyse the errors that are introduced by ML height variations, the CO contributions are also calculated using varying PBL heights. The absolute differences are integrated in time and the spatial distribution is represented in Fig. 6d by different colors. Since only negative values are found over Greece, the ML height variations cause an overestimation of the CO concentration at the receptor. This overestimation sums up to a total difference of $-9.6\,\mathrm{ppb}$ or $-16\,\%$.~~

For a more detailed analysis we spatially integrate the 3-d field of CO source contributions. Then, the total pick up of CO at each time step can be shown in a time series. Additionally, we also calculate the source contributions for the $100\,\mathrm{m}$ FL height and the dynamical layer that follows local PBL heights. In Fig. 7a, the pick up of CO contributions is shown for the time window when the Greek forest fires would have been passed by the trajectories. It reveals that the major pick up takes place over day between 6 and 15 UTC. The comparison between different FL height assumptions indicates similar CO values for the constant $100\,\mathrm{m}$ and $300\,\mathrm{m}$ FL height. They significantly exceed the values for the dynamical layers of the PBL and the fire plume top height.

At the peak of CO pick up at 11 UTC on 28th July, the CO contributions of the fire plume height and the PBL height are about $30\,\%$ below the level of the $100/300\,\mathrm{m}$ FL height. This is basically caused by the strong dilution of emitted CO in the deep layer of the fire plume respective PBL height. Both layers are about $1700\,\mathrm{m}$ with slightly higher values for the fire plume height. At night-time, the PBL heights are in the range of the fixed FL heights and the simulated CO source contributions are similar. We also analyse the time series of the density-weighted residence time $\widehat{T}$. In Fig. 7b, it is arranged next to the time series of CO contributions. It confirms that the residence time increases for deeper FL heights with the highest values for the fire plume and PBL height. However, this pronounced gain in impact is not sufficient to compensate for the strong dilution which results in lower CO contributions for both dynamical FL heights. In contrast to that, the $300\,\mathrm{m}$ simulation shows only a small gain in impact compared to the $100\,\mathrm{m}$ FL height that is almost compensated by the stronger dilution. Both constant FL heights have similar CO contributions of $676\,\mathrm{ppb}$ and $745\,\mathrm{ppb}$.

Overall, the $100\,\mathrm{m}$ FL height results in the highest CO contributions that exceeds the contribution from fire plume heights by $77\,\%$. The $300\,\mathrm{m}$ FL height yields $60\,\%$ and the PBL height $32\,\%$ more CO, see Tab. 3. Therefore, constant FL heights of $100-300\,\mathrm{m}$ significantly overestimate the emission impact in this meteorological situation.

Table 3. Total CO contributions for different footprint layer heights and relative differences in reference to the results of fire plume top heights.

New Table added

footprint height	CO contribution	relative difference
100 m	745 ppb	+77 %
300 m	676 ppb	+60 %
PBL	555 ppb	+32 %
fire plume height	420 ppb	-

~~To further analyse the impact of the diurnal cycle in PBL heights, the 3-d field of CO source contributions is spatially integrated. Then, the total pick up of CO at each time step is calculated and can be shown in a time profile. In Fig. 7a, this pick up of CO contributions is shown for the time window, when the Greek forest fires would have been passed by the trajectories. It reveals that the major pick-up takes place over day between 9 and 18 local time. This is accompanied by a negative difference of more than 20 % and hence a pronounced overestimation of CO contributions.~~

~~During this time window 12 hours prior at 28th July 12:00 UTC (15:00 local time), the PBL height reaches a mean daytime peak of 1500 m. Therefore, the stronger dilution decreases the concentration of emitted pollutants by 80 %. On the other hand, the residence time of trajectories captured within this layer increases and reinforces the total pick up of emissions.~~

~~For a detailed analysis of this interaction, the time profile of corresponding density-weighted residence time $\widehat{T}$ is calculated with eq. 2* and 4*. In Fig. 7b, it is arranged next to the time profile of CO contributions. It verifies that the residence time increases by more than twice at time step −12 h. However, this gain in impact is not sufficient to compensate the strong dilution. The CO contribution from the PBL height is lower than from a constant ML height of 300 m. Therefore, the neglected dilution can be identified as the driving mechanism that leads to an overestimation of emission impact. In addition, this effect is amplified, since the emission sources are passed in a time window with a pronounced negative difference in emission sensitivity.~~

4 Conclusions

In this study, we analysed the impact of different footprint layer (FL) height assumptions on the quantification of source contributions with the Lagrangian Particle Dispersion Model (LPDM) FLEXPART ~~have compared the source identification with the LPDM model FLEXPART for two different mixing layer (ML) height assumptions.~~ The FL height defines the vertical layer adjacent to the ground in which surface emissions are present and assumed to affect passing air tracer particles. Consequently, t~~T~~he assumed FL~~ML~~ height determines a~~the~~ dilution of any emitted pollutants ~~at ground level~~ and the number of ~~passing~~ trajectories ~~that are~~ exposed to the emissions. ~~Furthermore,~~ B~~b~~oth effects counteract each other: A growth in FL~~ML~~ height leads to a stronger dilution that is coupled to a stronger impact. ~~Therefore, the effects of this ML height assumption on the~~

~~quantification of upwind emission sources are subject to discussion. Here, we distinguish four different effects. In case of a growing ML height, we analyse the effect of~~

– ~~loss in concentration (dilution effect)~~

– ~~gain in impact.~~

~~In case of a decreasing ML height, the reverse effects of~~

– ~~gain in concentration~~

– ~~loss in impact~~

~~are analysed.~~ In a well-mixed layer with a homogeneous trajectory distribution and thus a constant tracer particle density, the counteracting effects are balanced. The dilution is in addition to the vertical mixing represented in the underlying meteorological model. It thus has the potential to compensate for any underestimation of vertical mixing in the trajectories. Then, FL height variations are buffered and the results of source quantification are independent of the FL height. Pan et al. (2014) found that FL height changes up to $300\,\mathrm{m}$ had no effect on the results. In fact, constant FL heights between $100\,\mathrm{m}$ and $300\,\mathrm{m}$ are used in most LPDM applications. However, mixing processes in the planetary boundary layer (PBL) have a pronounced spatio-temporal variability. Pollutants can be vertically diluted on timescales about $15\,\mathrm{min}$ within heights up to $2-3\,\mathrm{km}$. In these cases the PBL is well-mixed and its height can be used as a reference FL height that is independent of the vertical mixing represented by the trajectories. We explicitly use the local PBL heights as a dynamical FL height and compare the results to a constant FL height of $300\,\mathrm{m}$.

~~First, we used the recommended assumption of a constant ML height of $300\,\mathrm{m}$ that is close to the minimum of the planetary boundary layer (PBL) height (Seibert and Frank, 2004). This simplification assumes a constant dilution and decouples the two effects. Then, the sensitivity to emissions is proportional to the residence time of the trajectory ensemble in the ML and spatio-temporal independent. Additionally, this assumption lowers the risk to falsely consider trajectories outside the ML height. However, it fails to consider stronger dilution and influencing more trajectories in the convective ML during daytime. Then, we compared the source quantification of the $300\,\mathrm{m}$ ML height assumption to that of a spatio-temporal ML height. This variable ML height is realized by the PBL heights that are derived from the model. Since the PBL height follows a pronounced diurnal cycle, it provides a dynamic ML height that depends on local conditions and the time of the day. Hence, it is suited for the purpose here even though the modelled PBL height in FLEXPART is subject to uncertainties (Berkes, 2014).~~

For the comparison, we used in total 216 FLEXPART simulations that were carried out during the CYPHEX campaign at Cyprus in July 2014. The case studies provide different meteorological conditions and transport patterns. For convective conditions over day, the PBL heights significantly exceed the $300\,\mathrm{m}$ FL height assumption. Here, the increase in FL heights causes a decrease in source contributions by 6% on average. The variability of local conditions even allows for a decrease of more than 10%. The vertical mixing appears to be underrepresented in the trajectories and the technique of the fixed FL height assumption introduces an error. The overestimation of source contributions points out that Cyprus has a large impact from trajectories in lower levels. More trajectories in levels above $300\,\mathrm{m}$ would introduce an underestimation. In case of stable conditions typical for nocturnal PBL heights below $300\,\mathrm{m}$, there is almost no vertical mixing. Since the FLEXPART model uses a minimal PBL height of $100\,\mathrm{m}$, a minimum of vertical mixing within this layer is assumed. FL heights below this PBL minimum are not recommended to obtain good numerical stability (Seibert and Frank, 2004; Stohl et al., 2007b). On average over all case studies, we find a neglecting increase $< 1\%$ in source contributions for FL heights between $100 - 300\,\mathrm{m}$ compared to the fixed $300\,\mathrm{m}$ FL height. In this range, the FL height changes are buffered which is in agreement to the findings in Pan et al. (2014). However, the local variability allows for increases as well as decreases between $4 - 8\%$ with peaks of more than 15%. In both cases, the buffering fails due to an inhomogeneous tracer particle distribution in the $300\,\mathrm{m}$ FL height. The trajectories only represent the vertical mixing in FL heights within the PBL. FL heights should thus not exceed PBL heights for surface emissions (Stohl et al., 2007b). However, the situation is different for intensive vegetation fires. Here, the dynamics of the fire fuels convection leading to fire plume top heights that exceed local PBL heights.

~~With this variety, differences in emission sensitivity are quantified for different local conditions:~~

- ~~When the PBL height exceeds the $300\,\mathrm{m}$ height assumption, we observed a decrease in emission sensitivity by $5.9\,\%$ in average. The variability of local conditions allows for a decrease of $10\,\%$ and more. Positive differences of more than $3\,\%$ are rarely observed. Thus, the strong dilution in extended ML heights dominates the accompanied gain in impact. The $300\,\mathrm{m}$ ML assumption overestimates the impact of source regions due to this neglected dilution.~~

- ~~When the PBL height falls below $300\,\mathrm{m}$, a weak increase of $0.8\,\%$ is observed in average. It results from two counteracting effects. The gain in concentration is compensated by the accompanied loss in impact. Accordingly, the temporal and spatial variability reveals both an increase and a decrease in emission sensitivity of $4 - 8\,\%$ with outliers of more than $15\,\%$. The dominant effect depends strongly on the vertical distribution of air tracer particles in the lower troposphere. In a homogeneous vertical distribution, the gain in concentration dominates. Hence, the $300\,\mathrm{m}$ height assumption underestimates the impact of emission sources. In reverse, when air tracers agglomerate between the $300\,\mathrm{m}$ and the shallow PBL height below, they are falsely influenced within the $300\,\mathrm{m}$ height. Then, the gain in impact leads to a false identification of source regions and the $300\,\mathrm{m}$ assumption overestimates their impact.~~

~~Overall, the neglected dilution is identified as the major effect and the $300\,\mathrm{m}$ height assumption overestimates the impact of emission sources by $3 - 7\,\%$ in average.~~

For an application example, we arrange emission data of a strong fire event in Greece in August 2007 with our case study which happens to simulate long residence times that fire region. In 84% of the grid cells with fires, the fire plume top height exceeds the local PBL height. For the hypothetical case study, we compare the pick up of CO emissions within the fire plume height, the local PBL height and the constant FL heights of $300\,\mathrm{m}$ and $100\,\mathrm{m}$. The results show that the pick up of CO is the lowest for the application with fire plume heights. The total CO source contribution is about 77% higher for the $100\,\mathrm{m}$ FL height and 60% higher for the $300\,\mathrm{m}$ FL height assumption. This confirms that the results are not very sensitive to small changes in the FL height within $300\,\mathrm{m}$ (Pan et al., 2014; Stohl et al., 2007b). For local PBL heights, the total CO source contribution is about 32% higher than for fire plume heights. This overestimation is moderate compared to the constant FL height assumptions. The PBL height might thus be a reasonable assumption when fire plume heights are not available except for a very stable and shallow PBL heights. ~~So far, we discuss errors in the emission sensitivity that quantifies the relative impact of emission sources. However, the absolute impact of emission sources additionally depends on the source strength. The combination of emission sensitivity and emission flux density quantifies the contribution of upwind sources to the measured concentration at the receptor site. Hence, the errors amplify when strong emissions locally coincide with strong differences in emission sensitivity. This effect is confirmed in a typical application example of LPDMs (e.g., Forster et al., 2001; , 2007; , 2007a), that simulates the CO source contributions from forest fires. Here, the 300 m ML height assumption overestimates the pick up of CO emissions by 16 % on average and up to 20 % at single time steps.~~

~~Furthermore, we also discuss the assumption of a 100 m ML height. This shallow ML height is widely-used in applications of FLEXPART (e.g., Stohl et al., 2007a; , 2014), since it represents the PBL height minimum that is used in the model. Then, a false identification of trajectories above the PBL height is excluded. However, the neglected dilution in this shallow ML height amplifies the overestimation of source contribution and leads to a distinct negative bias.~~

From this study it can be concluded that the assumption of the FL~~ML~~ height in LPDMs is of vital importance for the relationship between emission sources and the atmospheric composition at the receptor site. While small variations in FL height up to 300 m are buffered to some extent, stronger variations cause major differences in the simulation of source contributions. In particular, for fire emission with variable plume heights exceeding local PBL heights, FL height assumptions below 300 m significantly over or underestimate the emission impact. We find an overestimation when the receptor has a large impact from lower levels close to the surface. In cases of a larger impact from upper levels, this turns into an underestimation. This error can affect two different applications: When source contributions from upwind emission sources to an observation point are quantified, their impact is over or underestimated. When the emission flux of sources is estimated that matches the measured concentration at the downwind observation point, the source strength is over or underestimated. This error might affect emission inventories derived from observations performed at long range. ~~Errors in ML height assumptions influence the emission sensitivity by the competing effects of loss / gain in concentration and gain / loss in impact. The weight of each effect depends on the ML height and the vertical distribution of air tracer particles. This is determined by the spatio-temporal variability in ML heights and the local meteorological conditions. They control the balance of both effects and finally the sensitivity to emission sources. The simplified assumption of a constant ML height close to the PBL height minimum neglects this spatio-temporal variability. Although the counteracting effects buffer these errors to some extent, the neglected dilution of emission fluxes introduces a major error in the quantification of emission sources. This affects two different applications: When source contributions from upwind emission sources to an observation point are quantified, their impact is overestimated. When the emission fluxes of sources is estimated that matches the measured concentration at the downwind observation point, the source strength is underestimated. These errors may be incorporated into emission inventories.~~ On a longer term, the option for the use of variable FL heights included to LPDMs is desirable. This is particularly of importance for the application on fire emissions with varying emission heights. All data are archived at the Max Planck Institute for Chemistry in Mainz and available on request. ~~a dynamic ML height parametrization derived from local varying PBL heights should be included to LPDM models used to analyse the relation between sources of emission flux and receptor concentrations.~~

Author contributions. I. Hüser conducted the FLEXPART simulations, data analysis and wrote the manuscript. H. Harder co-organized the CYPHEX campaign and supervised I. Hüser. A. Heil extracted data from ECMWF and co-wrote the manuscript. J. Kaiser provided CO emissions from GFASv1.2 and co-wrote the manuscript.

Acknowledgements. This study was conducted for the CYPHEX campaign and was funded by the Max Planck Society (MPG). The work on fire emissions was funded by the European Union through the CAMS_44 contract with ECMWF. Furthermore, we thank ECMWF for permitting access to the operational archive. ~~ANY IDEAS who needs to be in here ???~~

References

Andreae, M., Rosenfeld, D., Artaxo, P., Costa, A., Frank, G., Longo, K., and Silva-Dias, M. A. F.: Smoking Rain Clouds over the Amazon, Science, 303, 1337–1342, 2004.

Berkes, F.: Stabilität und Transport in der planetaren Grenzschicht - Untersuchungen mit Radiosonden- und Spurengasmessungen während PARADE, Ph.D. thesis, Johannes Gutenberg-Universität, 2014.

Dahlkötter, F., Gysel, M., Sauer, D., Minikin, A., Baumann, R., Seifert, P., Ansmann, A., Fromm, M., Voigt, C., and Weinzierl, B.: The Pagami Creek smoke plume after long-range transport to the upper troposphere over Europe – aerosol properties and black carbon mixing state, Atmospheric Chemistry and Physics, 14, 6111–6137, doi:10.5194/acp-14-6111-2014, http://www.atmos-chem-phys.net/14/6111/2014/, 2014.

Damoah, R., Spichtinger, N., Servranckx, R., Fromm, M., Eloranta, E., Razenkov, I., James, P., Shulski, M., Forster, C., and Stohl, A.: A case study of pyro-convection using transport model and remote sensing data, Atmospheric Chemistry and Physics, 6, 173–185, 2006.

Duck, T. J., Firanski, B. J., Millet, D. B., Goldstein, A. H., Allan, J., Holzinger, R., Worsnop, D. R., White, A. B., Stohl, A., Dickinson, C. S., and van Donkelaar, A.: Transport of forest fire emissions from Alaska and the Yukon Territory to Nova Scotia during summer 2004, Journal of Geophysical Research: Atmospheres, 112, n/a–n/a, doi:10.1029/2006JD007716, http://dx.doi.org/10.1029/2006JD007716, d10S44, 2007.

Forster, C., Wandinger, U., Wotawa, G., James, P., Mattis, I., Althausen, D., Simmonds, P., O'Doherty, S., Jennings, S. G., Kleefeld, C., Schneider, J., Trickl, T., Kreipl, S., Jäger, H., and Stohl, A.: Transport of boreal forest fire emissions from Canada to Europe, Journal of Geophysical Research: Atmospheres, 106, 22 887–22 906, doi:10.1029/2001JD900115, http://dx.doi.org/10.1029/2001JD900115, 2001.

Kaiser, J. W., Heil, A., Andreae, M. O., Benedetti, A., Chubarova, N., Jones, L., Morcrette, J.-J., Razinger, M., Schultz, M. G., Suttie, M., and van der Werf, G. R.: Biomass burning emissions estimated with a global fire assimilation system based on observed fire radiative power, Biogeosciences, 9, 527–554, doi:10.5194/bg-9-527-2012, 2012.

Kljun, N., Rotach, M., and Schmid, H.: A Three-Dimensional Backward Lagrangian Footprint Model For A Wide Range Of Boundary-Layer Stratifications, Boundary-Layer Meteorology, 103, 205–226, doi:10.1023/A:1014556300021, http://dx.doi.org/10.1023/A:1014556300021, 2002.

Lal, S., Venkataramani, S., Chandra, N., Cooper, O. R., Brioude, J., and Naja, M.: Transport effects on the vertical distribution of tropospheric ozone over western India, Journal of Geophysical Research: Atmospheres, 119, 10 012–10 026, doi:10.1002/2014JD021854, 2014JD021854, 2014.

Lelieveld, J., Evans, J. S., Fnais, M., Giannadaki, D., and Pozzer, A.: The contribution of outdoor air pollution sources to premature mortality on a global scale, Nature, 525, 367–371, doi:10.1038/nature15371, http://dx.doi.org/10.1038/nature15371, 2015.

Pan, X. L., Kanaya, Y., Wang, Z. F., Tang, X., Takigawa, M., Pakpong, P., Taketani, F., and Akimoto, H.: Using Bayesian optimization method and FLEXPART tracer model to evaluate CO emission in East China in springtime, Environmental Science and Pollution Research, 21, 3873–3879, doi:10.1007/s11356-013-2317-2, electronic supplementary material The online version of this article (doi: 10.1007/s11356-013-2317-2) contains supplementary material, which is available to authorized users., 2014.

Paugam, R., Wooster, M., Atherton, J., Freitas, S. R., Schultz, M. G., and Kaiser, J. W.: Development and optimization of a wildfire plume rise model based on remote sensing data inputs - Part 2, Atmospheric Chemistry and Physics Discussions, 15, 9815–9895, doi:10.5194/acpd-15-9815-2015, http://www.atmos-chem-phys-discuss.net/15/9815/2015/, 2015.

Poupkou, A., Markakis, K., N..Liora, Giannaros, T. M., Zanis, P., Im, U., Daskalakis, N., Myriokefalitakis, S., Kaiser, J. W., Melas, D., Kanakidou, M., Karacostas, T., and Zerefos, C.: A modeling study of the impact of the 2007 Greek forest fires on the gaseous pollutant levels in the Eastern Mediterranean, Atmos. Env., 148, 1–17, doi:10.1016/j.atmosres.2014.05.015, 2014.

Rémy, S., Veira, A., Paugam, R., Sofiev, M., Kaiser, J. W., Marenco, F., Burton, S. P., Benedetti, A., Engelen, R. J., Ferrare, R., and Hair, J. W.: Two global data sets of daily fire emission injection heights since 2003, Atmospheric Chemistry and Physics, 17, 2921–2942, doi:10.5194/acp-17-2921-2017, http://www.atmos-chem-phys.net/17/2921/2017/, 2017.

Rodean, H. C.: Stochastic Lagrangian Models of Turbulent Diffusion, Meteorological Monographs, 48, 1–84, doi:10.1175/0065-9401-26.48.1, http://dx.doi.org/10.1175/0065-9401-26.48.1, 1996.

Schmid, H. P.: Source areas for scalars and scalar fluxes, Boundary-Layer Meteorology, 67, 293–318, doi:10.1007/BF00713146, http://dx.doi.org/10.1007/BF00713146, 1994.

Seibert, P. and Frank, A.: Source-receptor matrix calculation with a Lagrangian particle dispersion model in backward mode, Atmospheric Chemistry and Physics, 4, 51–63, doi:10.5194/acp-4-51-2004, http://www.atmos-chem-phys.net/4/51/2004/, 2004.

Stohl, A.: Computation, accuracy and applications of trajectories - A review and bibliography, Atmospheric Environment, 32, 947 – 966, doi:http://dx.doi.org/10.1016/S1352-2310(97)00457-3, 1998.

Stohl, A. and Thomson, D. J.: A density correction for Lagrangian particle dispersion models, Bound.-Lay, Meterol, pp. 155–167, 1999.

Stohl, A., Hittenberger, M., and Wotawa, G.: Validation of the Lagrangian particle dispersion model FLEXPART against large scale tracer experiment data, Atmos, Environ, 1998.

Stohl, A., Eckhardt, S., Forster, C., James, P., Spichtinger, N., and Seibert, P.: A replacement for simple back trajectory calculations in the interpretation of atmospheric trace substance measurements, Atmospheric Environment, 36, 4635 – 4648, doi:http://dx.doi.org/10.1016/S1352-2310(02)00416-8, 2002.

Stohl, A., Forster, C., Frank, A., Seibert, P., and Wotawa, G.: Technical note: The Lagrangian particle dispersion model FLEXPART version 6.2, Atmospheric Chemistry and Physics, 5, 2461–2474, doi:10.5194/acp-5-2461-2005, http://www.atmos-chem-phys.net/5/2461/2005/, 2005.

Stohl, A., Berg, T., Burkhart, J. F., Fjaeraa, A. M., Forster, C., Herber, A., Hov, O., Lunder, C., McMillan, W. W., Oltmans, S., Shiobara, M., Simpson, D., Solberg, S., Stebel, K., Ström, J., Torseth, K., Treffeisen, R., Virkkunen, K., and Yttri, K. E.: Arctic smoke - record high air pollution levels in the European Arctic due to agricultural fires in Eastern Europe in spring 2006, Atmospheric Chemistry and Physics, 7, 511–534, doi:10.5194/acp-7-511-2007, http://www.atmos-chem-phys.net/7/511/2007/, 2007a.

Stohl, A., J. F. Burkhart, S. E., Hirdman, D., and Sodemann, H.: An integrated internet-based system for analyzing the influence of emission sources and atmospheric transport on measured concentrations of trace gases and aerosols, Tech. rep., Norwegian Institute for Air Research, Kjeller, Norway, 2007b.

Stohl, A., Seibert, P., Arduini, J., Eckhardt, S., Fraser, P., Greally, B. R., Lunder, C., Maione, M., Mühle, J., O'Doherty, S., Prinn, R. G., Reimann, S., Saito, T., Schmidbauer, N., Simmonds, P. G., Vollmer, M. K., Weiss, R. F., and Yokouchi, Y.: An analytical inversion method for determining regional and global emissions of greenhouse gases: Sensitivity studies and application to halocarbons, Atmospheric Chemistry and Physics, 9, 1597–1620, doi:10.5194/acp-9-1597-2009, http://www.atmos-chem-phys.net/9/1597/2009/, 2009.

Stull, R.: An Introduction to Boundary Layer Meteorology, Atmospheric and Oceanographic Sciences Library, Springer Netherlands, 1988.

Stull, R.: 9 - The Atmospheric Boundary Layer, in: Atmospheric Science (Second Edition), edited by Wallace, J. M. and Hobbs, P. V., pp. 375 – 417, Academic Press, San Diego, second edition edn., doi:https://doi.org/10.1016/B978-0-12-732951-2.50014-4, http://www.sciencedirect.com/science/article/pii/B9780127329512500144, 2006.

Tyrlis, E., Tymvios, F. S., Giannakopoulos, C., and Lelieveld, J.: The role of blocking in the summer 2014 collapse of Etesians over the eastern Mediterranean, Journal of Geophysical Research: Atmospheres, pp. n/a–n/a, doi:10.1002/2015JD023543, 2015JD023543, 2015.

Van Dam, B., Helmig, D., Burkhart, J. F., Obrist, D., and Oltmans, S. J.: Springtime boundary layer O3 and GEM depletion at Toolik Lake, Alaska, Journal of Geophysical Research: Atmospheres, 118, 3382–3391, doi:10.1002/jgrd.50213, http://dx.doi.org/10.1002/jgrd.50213, 2013.

Vardoulakis, S. and Kassomenos, P.: Sources and factors affecting PM10 levels in two European cities: Implications for local air quality management, Atmospheric Environment, 42, 3949 – 3963, doi:http://dx.doi.org/10.1016/j.atmosenv.2006.12.021, http://www.sciencedirect.com/science/article/pii/S1352231006012301, fifth International Conference on Urban Air Quality, 2008.

Vogelezang, D. and Holtslag, A.: Evaluation and model impacts of alternative boundary-layer height formulations, Boundary-Layer Meteorology, 81, 245–269, doi:10.1007/BF02430331, 1996.

New Figure added

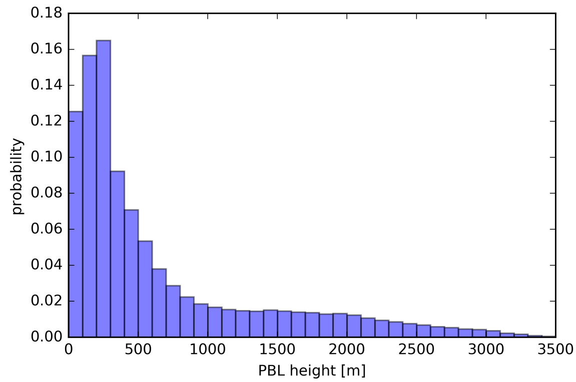

Figure 1. Frequency distribution of PBL heights occurring during the 5 days backward simulation from 19th July 2014 00 UTC+03.

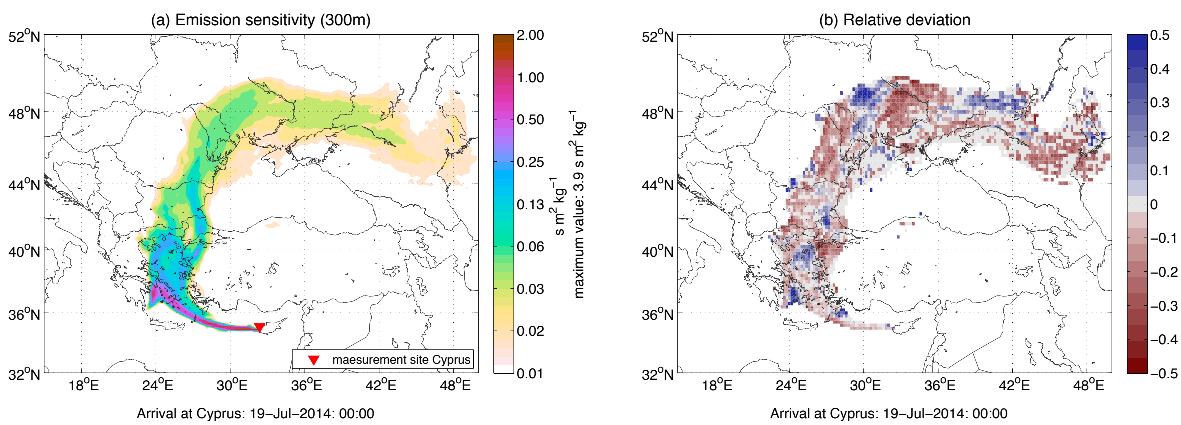

Figure 2. (a) Time integrated emission sensitivity referring to the constant $300\,\mathrm{m}$ footprint~~mixing~~ layer height assumption for a 5 day backward simulation started on 19th July 2014 00 UTC+03 at Cyprus. Sensitivities below $0.01\,\mathrm{s\,m^{-2}\,kg^{-1}}$ are not considered. (b) Relative difference in emission sensitivity introduced by differences between local boundary layer heights and the constant $300\,\mathrm{m}$ footprint~~mixing~~ layer height. Only absolute sensitivity differences above $0.0025\,\mathrm{s\,m^{-2}\,kg^{-1}}$ are used to calculate relative differences.

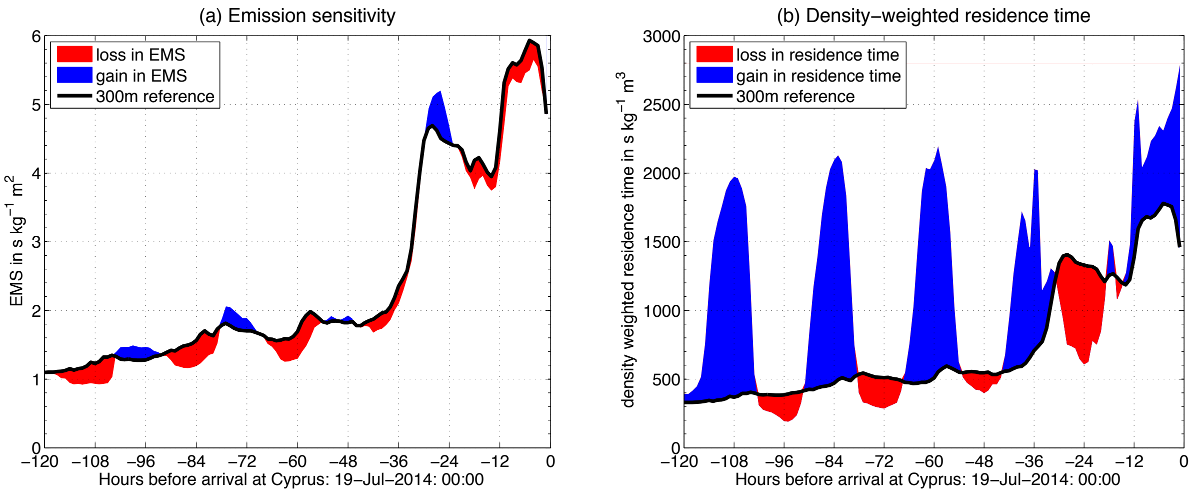

Figure 3. (a) Time profile~~series~~ of spatially integrated emission sensitivity (EMS) based on variable boundary layer heights with positive differences (blue areas) and negative (red areas) in reference to the 300 m assumption (black line). (b) Spatially integrated density-weighted residence time of boundary layer heights with differences shown by filled areas in respect to the 300 m layer.

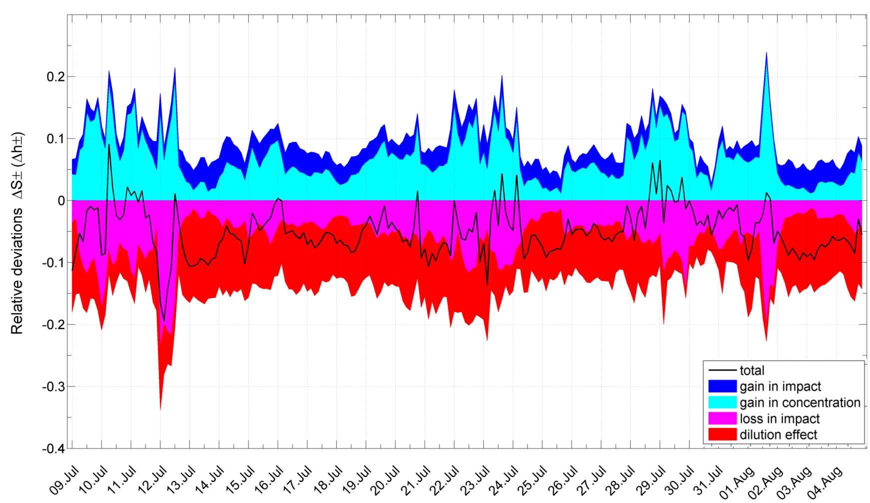

legend corrected

Figure 4. Temporal changes in the overall difference in emission sensitivity ΔS_{tot} enveloped by the positive and negative contributions that correspond to increase / decrease in footprint~~mixing~~ layer height $\Delta h\pm$ and the defined effects of Eq. 8~~11~~ based on 216 simulations. Differences by footprint~~mixing~~ layer variations are calculated relatively in reference to the constant 300 m assumption.

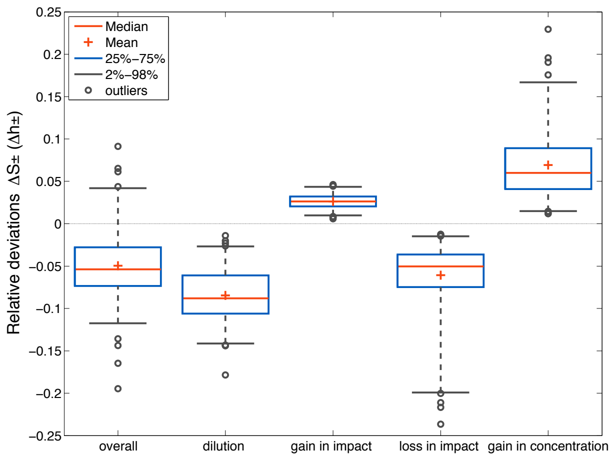

Figure 5. Box whisker plot for the overall differences in emission sensitivity and the contributions of the different effects in reference to the $300\,\mathrm{m}$ assumption based on 216 simulation. The whisker ends are defined by the 2nd and 98th percentile and remaining outliers considered by outlying circles.

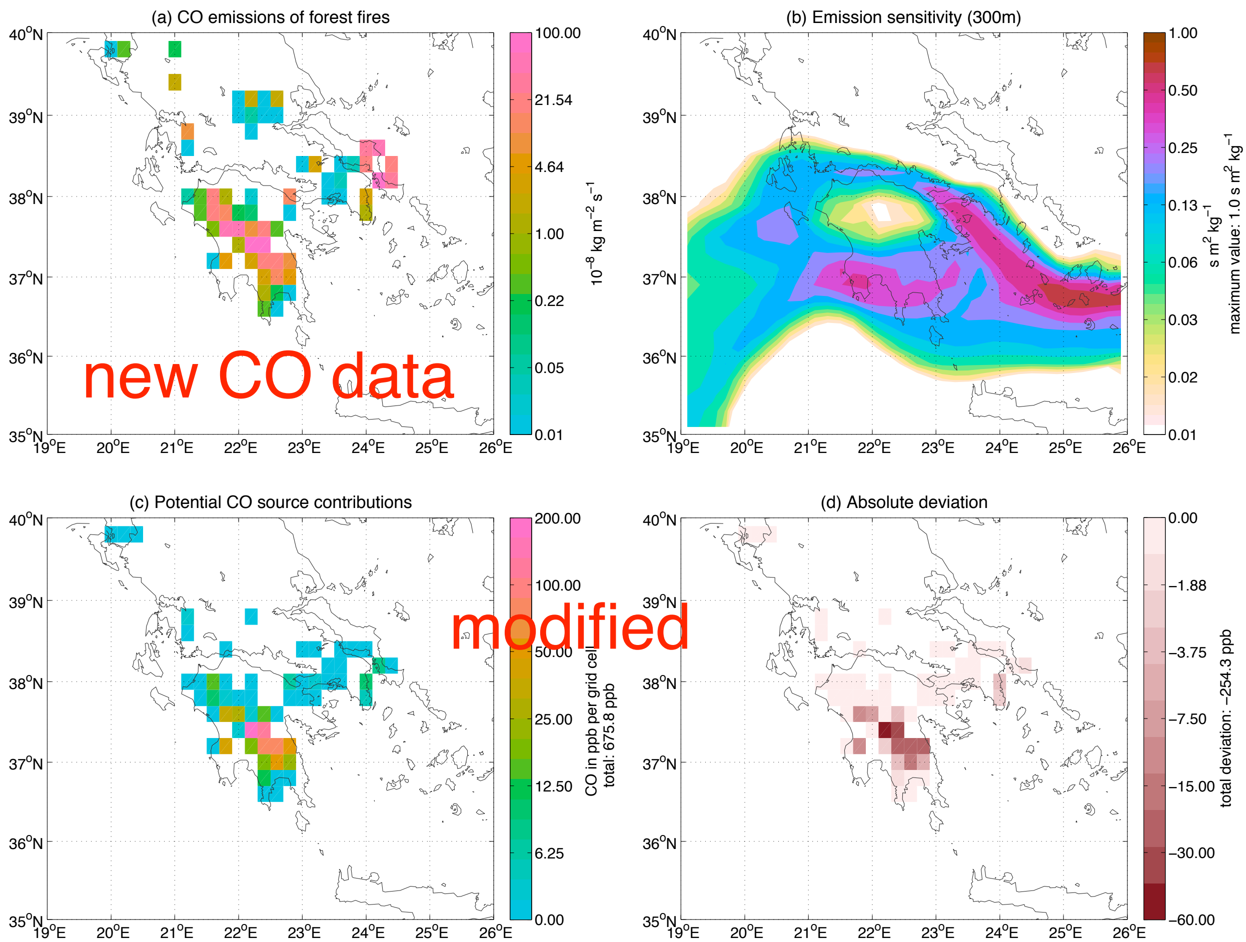

Figure 6. (a) CO emissions for forest fires in Greece on 26th~~as a monthly mean for~~ August 2007 provided by GFASv1.2 (Kaiser et al., 2012) and aggregated~~extrapolated~~ on a grid of 0.2°. (b) ~~Zoom in the region of Greek forest fires for the~~ Ttime-integrated emission sensitivity of a 5 day backward simulation from 30th July 2014 15 UTC+3 started at Cyprus and based on the 300 m footprint~~mixing~~ layer height. (c) ~~Time-integrated potential~~ CO source contributions of forest fires to~~in~~ mass mixing ratio at Cyprus assuming a ~~within the~~ 300 m footprint layer height and (d) absolute differences introduced by using variable fire plume heights as footprint layer height ~~mixing layer variations~~.

Figures modified

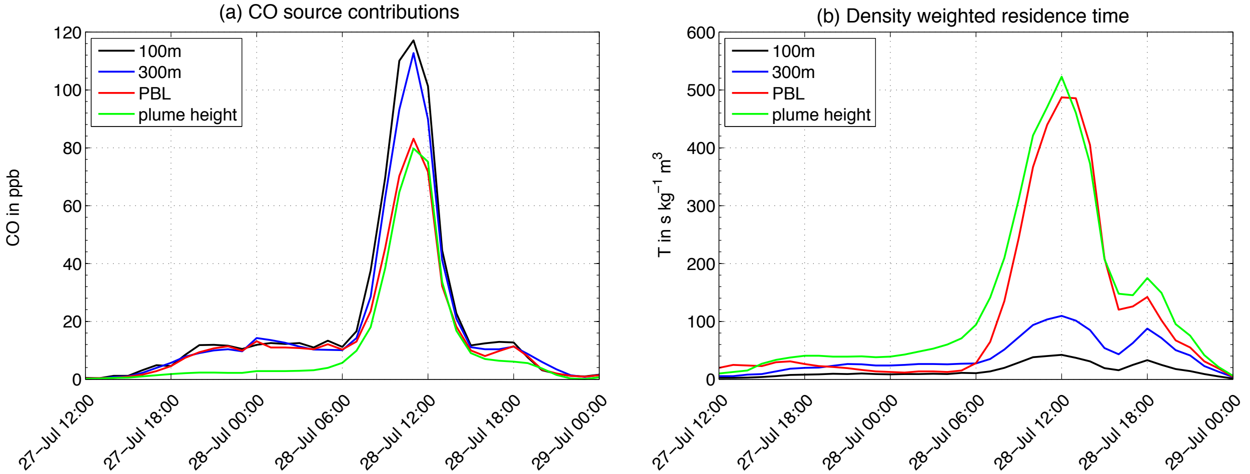

Figure 7. (a) Time series of spatial integrated CO source contributions for the different footprint layer heights and (b) the corresponding series of density-weighted residence time for the time window when Greek forest fires were passed.~~(a) Time profile of spatial integrated CO source contribution for the constant 300 m layer with differences introduced by mixing layer variations and (b) the corresponding profile of density-weighted residence time for the time window when Greek forest fires were passed. At 28-Jul 12:00 UTC a difference of −26 % in CO contribution is accompanied by a mean boundary layer height of 1500 m and an increase of 226 % in residence time.~~